Localized tail state distribution and hopping transport in ultrathin zinc-tin-oxide thin film transistor

Li, Jeng-Ting; Liu, Li-Chih; Chen, Jen-Sue; Jeng, Jiann-Shing; Liao, Po-Yung; Chiang, Hsiao-Cheng; Chang, Ting-Chang; Nugraha, Mohamad Insan; Loi, Maria

Published in:
Journal of Materials Research

DOI:
10.1063/1.4973992

Publication date:
2017

Localized tail state distribution and hopping transport in ultrathin zinc-tin-oxide thin film transistor

Jeng-Ting Li[1], Li-Chih Liu[1], Jen-Sue Chen[1]*, Jiann-Shing Jeng[2], Po-Yung Liao[3], Hsiao-Cheng Chiang[3], Ting-Chang Chang[3], Mohamad Insan Nugraha[4] and Maria Antonietta Loi[4]

[1]*Department of Materials Science and Engineering, National Cheng Kung University, Tainan 70101, Taiwan*

[2]*Department of Materials Science, National Tainan University, Tainan 70005, Taiwan*

[3]*Department of Physics, National Sun Yat-Sen University, Kaohsiung 804, Taiwan*

[4]*Zernike Institute for Advanced Materials, University of Groningen, Nijenborgh 4, Groningen 9747AG, The Netherlands*

**** Electronic mail:*** *jenschen@mail.ncku.edu.tw*

Abstract

Carrier transport properties of solution processed ultra thin (4 nm) zin-tin oxide (ZTO) thin film transistor are investigated based on its transfer characteristics measured at the temperature ranging from 310K to 77K. As temperature decreases, the transfer curves show a parellel shift toward more postive voltages. The conduction mechanism of ultra-thin ZTO film and its connection to the density of band tail states

have been substantiated by two approaches, including fitting logarithm drain current (log I_D) to $T^{-1/3}$ at 310K to 77K according to two-dimensional Mott variable range hopping theory and the extraction of density of localized tail states through the energy distribution of trapped carrier density. The linear dependency of log I_D vs. $T^{-1/3}$ indicates that the dominant carrier transport mechanism in ZTO is variable range hopping. The extracted value of density of tail states at the conduction band minimum is 4.75×10^{20} $cm^{-3}eV^{-1}$ through the energy distribution of trapped carrier density. The high density of localized tail states in the ultra thin ZTO film is the key factor leading to the room-temperature hopping transport of carriers among localized tail states.

Introduction

Amorphous oxide semiconductor (AOS) thin film transistors (TFTs) has been extensively research due to their advantages such as high optical transparency, relatively high electron mobility and low temperature processing techniques so that AOS could be used as transparent and flexible backplanes[1]. As well-known, the disordered amorphous semiconductors have high density of states (DOS) exist within the energy band gap, which will strongly affect the charge transport properties and mobility[2]. Several groups have studied the carrier transport properties in IGZO at room temperature is dominates by trap-limited conduction[3] as well as percolation[4],

which are both band like transport above the mobility edges. At low temperatures, electrons are constrained to the localized states around the Fermi level (E_F)[5] but cannot be excite electrons to conduction band owing to low thermal energy. Consequently, electrons must hop among the localized states around E_F and the charge transport mechanism is variable range hopping (VRH)[6]. In recent years, advanced AOSTFT devices pursue thinner active layer thickness, which is representative of electron transport in two-dimensional systems and the band tail states in AOS will be more significant. Considering a disordered material with very thin thickness and high density of localized states, carriers may be conducted through the localized states[7]. Consequently, the carrier transport process in AOS TFTs becomes complex and is worthy of in deep investigation.

In this work, zinc-tin oxide (ZTO) is chosen as the TFT active layer owing to its low-cost competency as compared with IGZO. ZTO is deposited by a solution process to form a uniform and ultra-thin active layer. We have combined two approaches to resolve the conduction mechanism of ultra-thin ZTO film and its connection to the density of band tail states. Firstly, it is demonstrated the hopping conduction mechanism is dominant for carrier transport in ultra-thin ZTO TFT by the linear dependency of log I_D vs. $T^{-1/3}$ over a temperature range (T=310~77K). Furthermore, based on the temperature-dependent measurement, the hopping density of localized

states (i.e. the density of band tail states) is derived through two-dimensional Mott VRH theory. For the second approach, we calculated the density of trapped carriers as a function of the surface potential (E_F-E_C) based on the charge induction by band bending at T=310 K and it can be used to extract the density of localized tail states. Our result suggests that the variable range hopping mechanism dominates the charge transport in solution process ZTO TFT from 77 K to room temperature.

Experimental

A bottom gate TFT stack was fabricated on the p^+-Si substrate (as gate electrode) covered with a 100 nm-thick SiO_2 layer (as gate dielectric). The ZTO active layer was prepared by a solution process with tin chloride and zinc acetate precursors (molar ratio of Zn:Sn=1:1) in the solvent of ethylene glycol monomethyl ether as described in reference[8]. The ZTO precursor solution was spin-coated on the SiO_2/Si substrate and annealed in air at 500 ^oC to form ZTO active layer with thickness of 4 nm. A 300 nm-thick Al were deposited by e-beam evaporation through a shadow mask to define the source/drain electrodes as well as the channel width (2000 μm) and length (100 μm). High-resolution transmission electron microscopy (HRTEM) images were obtained by using a JEM 2100F field-emission transmission electron microscope, and TEM sample were prepared by a focus ion beam system (SII SMI 3050). The TFT transfer curves (drain current (I_D) vs. gate voltage (V_G)) were measured by using

Agilent B1500 A semiconductor parameter analyzer in a cryogenic probe station (Lakeshore TTPX) under vacuum ambient with the temperature ranging between 77K and 310K.

Results and discussion

Fig. 1 show the cross-sectional TEM micrograph of solution processed ZTO film. Note that the TEM specimen was prepared by spin-coating the ZTO precursor solution onto a thin 10 nm SiO_2 grown on Si substrate and covered with an Al protection layer. As measured from the micrograph the thickness of ZTO film is about 4 nm and the image contrast suggests ZTO is amorphous-like. In addition, the grazing incidence X-ray diffraction data for 4nm ZTO film do not show diffraction peak at two-theta angles of 20^o-80^o, indicating that the solution processed ZTO thin film is essentially amorphous (see section S1 in supplementary material**)**. The thin ZTO and long channel length (100 μm) possibly leads to a relatively high channel resistance as compared to the contact resistance (the Al/ZTO junction is an Ohmic contact according to their work function difference, see section S2 in supplementary material). Therefore, the channel resistance shall be dominant in our electrical analysis and the influence of contact resistance may be ignored.

To determine the conduction mechanism of the ZTO active layer, the drain current of ZTO TFT measured at 310 K to 77K is analyzed. Fig. 2 (a) shows the

hysteresis I_D-V_G curves of the ZTO TFT measured at 310K and 77K. The device was characterized in high vacuum (3×10^{-5} torr) in order to avoid any influences in the atmosphere. The clockwise hysteresis I_D-V_G curve is obtained by sweeping V_G in the forward (-20 V to +40 V) -to-reverse (+40 V to -20 V) voltage direction. The hysteresis window is very small (< 1 V), which suggests no interface trap states between SiO_2 and ZTO[9]. In addition, the narrow hysteresis window indicates the V_G sweep range will not influence the TFT operation process. Fig. 2 (b) shows the I_D-V_G curves of the ZTO TFT under operating temperatures from 310K to 77K. The threshold voltages are shifted to more positive values with decreasing operating temperature while electron mobilty decreases slighty (see Sec. S3 in supplementary material). It can be explained by the reduction of thermally excited carriers at lower temperatures[10]. Consequently, the threshold voltage needed for carrier accumulation in ZTO active layer at low temperature increases.

In two-dimensional (2D) systems, the temperature dependence of the 2D VRH conduction by Mott is given by[11]

$$I_D = I_{D0}\exp(-\frac{B}{T^{1/3}}), \quad (1)$$

where I_{D0} is the drain current prefactor and B is a material constant (see discussion later). Fig. 3 (a) and (b) depict the log I_D vs. $T^{-1/3}$ curves at above-threshold (V_G above V_{TH}=-1.35 V) and sub-threshold (V_G=-10.72~-1.35 V) regions of ZTO TFT,

respectively. All log I_D vs. $T^{-1/3}$ curves exhibit linear dependency, indicating that the variable range hopping should be the dominant electrical transport mechanism in ZTO for both above-threshold and sub-threshold regions[12].

The transport mechanisms of channel electrons are discussed based on distribution of conducting carriers within the energy band gap of ZTO. From the distribution of conducting carriers, we can further determine the density of tail states. The carrier concentration in ZTO semiconductor can be calculated by following Lee and Nathan's derivation[13]**.** As first step, the conduction carrier density (n_{cond}) in ZTO TFT should be defined. The conduction carrier density as a function of gate voltage ($n_{cond}(V_G)$) is extracted from the measured I_D-V_D characteristics[13, 14],

$$n_{cond}(V_G) = \frac{1}{\varepsilon_s kT}\left(\frac{LI_D(V_G)}{\mu W V_D}\right)^2, \quad (2)$$

where μ is the mobility of the ZTO layer, ε_S the permittivity of semiconductor (the ε_S of a-IGZO[15] is put in since ε_S of ZTO is not available), k is the Boltzmann constant, T is the absolute temperature, W and L are the channel width the channel length, $I_D(V_G)$ is the drain at given V_G, and V_D is the drain voltage. Next, the V_G and E_F (the Fermi level of ZTO) can be correlation by a mapping function[13, 14],

$$E_F - E_C = 2kT\ln\left(\frac{I_D(V_G)}{\sqrt{N_C \varepsilon_S kT\mu(W/L)V_D}}\right), \quad (3)$$

where E_C is the conduction band minimum at ZTO/dielectrics interface, N_C is effective density of states for free carriers which is about $5\times10^{18}cm^{-3}$.[2] Based on these

parameters and equation (3), we analytically compute the correspondence of V_G with E_F-E_C of ZTO TFT at off-state, sub- threshold and above- threshold at 310 K, where the lowest E_F-E_C point represents the TFT in the flat band condition (see section S4 in supplementary material). Since the minimum E_F-E_C is -0.88 eV, it indicates that the Fermi level lies 0.88 eV below the conduction band minimum.

Next, we should define the density of trapped carriers (n_{trap}) at localized states. The n_{trap} and n_{cond} can be related to the electric potential of the semiconductor (i.e., the channel), which can be derived with Poisson's equation[13, 14],

$$\frac{d^2\varphi}{dx^2} = \frac{q}{\varepsilon_S}(n_{cond} + n_{trap}), \tag{4}$$

$$E = -\frac{d\varphi}{dx}, \tag{5}$$

where x is the distance from the semiconductor/dielectric interface along the channel depth, and φ the semiconductor potential along x, E is electric field. The carrier densities can be connected to gate voltage using a charge balance equation: $Q_{ind}=C_{ox}(V_G-V_{TH})$. Here, Q_{ind} is the total induced charge density at semiconductor/dielectric interface; C_{ox} is the gate-insulator capacitance, where V_{TH} is a threshold voltage. This yields the following[13, 14]:

$$E(x=0) = \sqrt{\frac{2q}{\varepsilon_S}\int_0^{\varphi_S}(n_{cond} + n_{trap})d\varphi} \approx \frac{C_{ox}(V_G - V_{TH})}{\varepsilon_S}, \tag{6}$$

Squaring equation (6) and taking its first derivative with respect to the surface

potential $\varphi(x = 0) = \varphi_S$, and $q\varphi_S = E_F - E_{F0}$, where E_F is the Fermi level position at surface, E_{F0} is an equilibrium Fermi level. Therefore, n_{trap} can be computed as[13, 14],

$$n_{trap} = \frac{\varepsilon_S}{2q}\frac{dE^2}{d\varphi_S} - n_{cond} . \quad (7)$$

Fig. 4 exhibits density of the conduction carriers and density of the trapped carriers as a function of E_F-E_C at the ZTO/dielectrics interface. The band gap of ZTO is 3.7 eV, as evaluated from the absorption edge of the UV-Vis spectrum (see Sec. S5 in supplementary material). The carrier densities are extracted from the transfer curve measured at T=310K. From equation (3), we have realized the E_C-E_F is determined from the magnitude of the gate bias, which indicates the extent of band bending. According to Fig. 4, density of the trap carriers is higher than the conduction carrier density, suggesting that huge localized tail states below E_C and the only few electrons could be excited by thermal energy to the upper conduction band minimum[13].

Based on equations (6), and (7), the density of localized tail states ($N_{tail,trap}(E)$) can be given as equation (8) [13, 14],

$$N_{tail,trap}(E) = \frac{dn_{trap}}{d\varphi_s} , \quad (8)$$

Fig. 5 shows the distribution of the density of localized tail states vs. E-E_C, in which the solid square curve is derived from equation (8). By fitting $N_{tail,trap}(E)$ to an exponential function of E-E_C, the tail state density at conduction band minimum, $N_{tc,trap}$, is retrieved, which follows[13, 14]

$$N_{tail}(E) = N_{tc} \exp(\frac{E - E_C}{kT_t}), \quad (9)$$

where kT_t is the characteristic tail state energy. In this work, the retrieved values of $N_{tc,trap}$ and kT_t are 4.75×10^{20} $cm^{-3}eV^{-1}$ and 78.8 meV, respectively for ZTO TFT. In particular, the extracted kT_t is much higher then kT (25.9 mV) at 310K; therefore, the free carrier becomes negligible[14].

From above analyses, we can find out that at the ZTO/dielectric interface, trapped carriers occupy the localized tail states below Fermi level at T=310K. This implies the good opportunity of carriers transport through unoccupied localized tail states above Fermi level[12]. This result echoes the linear dependency of log I_D vs. $T^{-1/3}$ curves, indicating that the variable range hopping should be the dominant electrical transport mechanism in ZTO.

The slope of log I_D vs. $T^{-1/3}$ curve is related to the constant B in equation (1) and B is given by[11]

$$B = \{\frac{2\alpha^2}{kN_{tail,VRH}(E)}\}^{1/3}, \quad (10)$$

where α is the inverse of the Bohr radius (a), k is Boltzmann's constant, and $N_{tail,VRH}(E)$ is the density of localized tail states. The Bohr radius (a) is calculated from: $a=\frac{a_0\varepsilon_s}{m^*/m_0}$, where a_0 is the Bohr radius of hydrogen atom (0.53Å), ε_s is the permittivity of semiconductor, m^* is the electron effective mass ($m^*=0.34\ m_0$, which is the value for a-IGZO)[4], and m_0 is the free electron mass). Fig. 5 also shows the

distribution of the localized tail states extracted from Mott VRH theory, $N_{tail,VRH}(E)$, in the solid circle curve. The $N_{tail,VRH}(E)$ can also be fitted to equation (9), yielding $N_{tc,VRH}$ and kT_t are 2.9×10^{18} $cm^{-2}eV^{-1}$ and 84.6 meV respectively. In the basic device theory, the transistor's operation is based on the accumulation of electrons at the oxide-semiconductor interface. The high $N_{tc,VRH}$ value leads to hopping conduction of electrons in two dimensional accumulation channel.

In a study on different types of transport mechanisms in IGZO layers, the authors demonstrated the contribution of the VRH conduction becomes greater than band-like conduction if the Fermi level E_F lies within exponential tail states with a characteristic temperature T_t around 800 K (equivalent to kT_t=69meV) and a tail state density at conduction band minimum in the order of 3.4×10^{19} cm^{-3} eV^{-1}.[16] Our extracting values of $N_{tc,trap}$ and T_t are higher than the numbers reported in previous study. Therefore, in our case, VRH mechanism seems to be the predominant mechanism in ZTO. This result is confirmed by the liner dependence of the logarithm of the log I_D vs. $T^{-1/3}$ observed in Fig. 3. In this work, the ZTO thin film is coated by a solution process and only 4 nm thick, which usually contains a lot of defects. It is therefore conceivable that the VRH governs the conduction in solution processed ZTO ultra-thin film at temperature range from 77K to 310 K.

Conclusion

The electrical properties of TFT with a 4 nm thick ZTO active layer are examined as function of temperature from 310K to 77K. According to the two dimensional Mott theory, the VRH mechanism dominates the charge transport in solution process ZTO active layer by linear dependency of log (I_D) vs. $T^{-1/3}$. Since $n_{trap}>n_{cond}$ at all surface potentials, charge transport at T=310 K is not dominated by conduction carriers in ZTO, but governed by variable range hopping of trapped carriers among localized tail states. Furthermore, the large density of localized tail states (~10^{20} $cm^{-3}eV^{-1}$ at the conduction band minimum) is extracted from the energy distribution of n_{trap} at T=310 K. The hopping conduction in ZTO channel layer can be explained by a considerably large amount of defects in ultra-thin, solution processed ZTO thin film, which is also evidenced by inferior charge-carrier mobility as compared to crystalline semiconductors.

Supplementary material

See supplementary material for discussion of contact resistance, ZTO band gap and additional data analysis.

Acknowledgements

The authors gratefully acknowledge the financial support from the Ministry of Science and Technology of Taiwan (Grant No. MOST 102-2221-E-006-071-MY3, and MOST 103-2221-E-006-086-MY3).

References

1. E. M. C. Fortunato, P. M. C. Barquinha, A. C. M. B. G. Pimentel, A. M. F. Gonçalves, A. J. S. Marques, L. M. N. Pereira, and R. F. P. Martins, Advanced Materials **17** (5), 590 (2005).

2. T. Kamiya, K. Nomura, and H. Hosono, Journal of Display Technology **5** (12), 468 (2009).

3. S. Lee, K. Ghaffarzadeh, A. Nathan, J. Robertson, S. Jeon, C. Kim, I. H. Song, and U. I. Chung, Applied Physics Letters **98** (20), 203508 (2011).

4. A. Takagi, K. Nomura, H. Ohta, H. Yanagi, T. Kamiya, M. Hirano, and H. Hosono, Thin Solid Films **486** (1), 38 (2005).

5. S. Lee, A. Nathan, J. Robertson, K. Ghaffarzadeh, M. Pepper, S. Jeon, C. Kim, I. H. Song, U. I. Chung, and K. Kinam, Electron Devices Meeting (IEDM), 2011 IEEE International, 14.6.1 (2011).

6. N. F. Mott, Journal of Non-Crystalline Solids **1** (1), 1 (1968).

7. I. I. Fishchuk, A. Kadashchuk, A. Bhoolokam, A. de Jamblinne de Meux, G. Pourtois, M. M. Gavrilyuk, A. Köhler, H. Bässler, P. Heremans, and J. Genoe, Physical Review B **93** (19), 195204 (2016).

8. L. C. Liu, J. S. Chen, J. S. Jeng, and W. Y. Chen, ECS Journal of Solid State Science and Technology **2** (4), Q59 (2013).

9. Y. J. Chen and Y. H. Tai, ECS Solid State Letters **4** (4), Q10 (2015).

10. C. Chen, K. Abe, H. Kumomi, and J. Kanicki, IEEE Transactions on Electron Devices **56** (6), 1177 (2009).

11. N. Mott, M. Pepper, S. Pollitt, R. H. Wallis, and C. J. Adkins, Proceedings of the Royal Society of London. Series A **345** (1641), 169 (1975).

12. Y. L. Huang, S. P. Chiu, Z. X. Zhu, Z. Q. Li, and J. J. Lin, Journal of Applied Physics **107** (6), 063715 (2010).

13. S. Lee and A. Nathan, Applied Physics Letters **101** (11), 113502 (2012).

14. S. Lee, A. Nathan, Y. Ye, Y. Guo, and J. Robertson, Scientific Reports **5**, 13467 (2015).

15. D. H. Lee, K. Nomura, T. Kamiya, and H. Hosono, ECS Solid State Letters **1** (1), Q8 (2012).

16. W. C. Germs, W. H. Adriaans, A. K. Tripathi, W. S. C. Roelofs, B. Cobb, R. A. J. Janssen, G. H. Gelinck, and M. Kemerink, Physical Review B **86** (15), 1555319 (2012).

Figure Captions

FIG. 1. Cross-sectional TEM image of spin-coated ZTO film on SiO_2 (10 nm)/p^+-Si. The surface is covered with an Al protection layer.

FIG. 2. (a) Hysteresis I_D-V_G curves of the ZTO TFT at 310K and 77K. (b) Transfer characteristics of ZTO TFT measured in the temperature range from 310K down to 77K.

FIG. 3. Plot of logarithm of drain current (I_D) vs. $T^{-1/3}$ at various operation regions for ZTO TFT, (a) above-threshold ($V_G > V_{TH} = -1.35$ V), (b) sub-threshold ($V_G < -1.35$ V).

FIG. 4. Plot of conduction carrier density and trapped carrier density of ZTO TFT at 310K as a function of E_F-E_C.

FIG. 5. The distribution of the density of localized tail states vs. E-E_C in ZTO TFT, extracted using Lee and Nathan's derivation and 2D Mott's variable range hopping method. The dash line indicates the exponential profile of density of localized tail states, which follows $N_{tail}(E)=N_{tc}\exp[E-E_C)/kT_t]$.

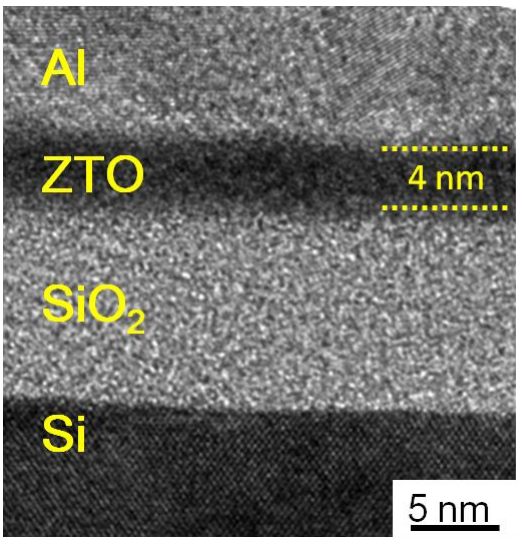

FIG. 1. Cross-sectional TEM image of spin-coated ZTO film on SiO_2 (10 nm)/p^+-Si. The surface is covered with an Al protection layer.

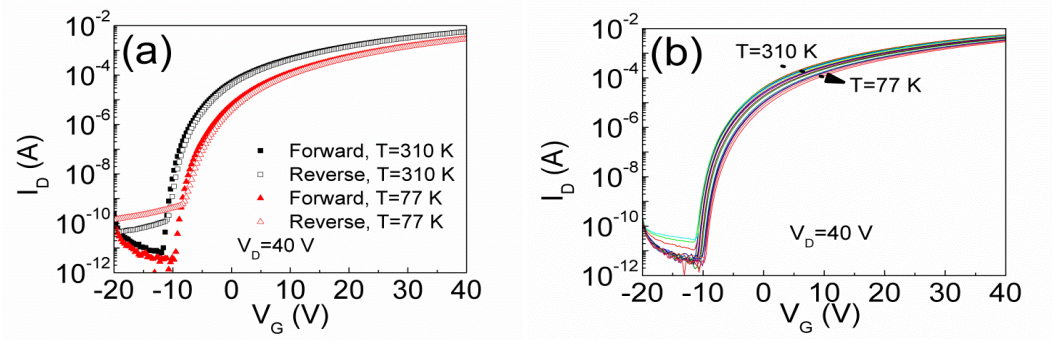

FIG. 2. (a) Hysteresis I_D-V_G curves of the ZTO TFT at 310K and 77K. (b) Transfer characteristics of ZTO TFT measured in the temperature range from 310K down to 77K.

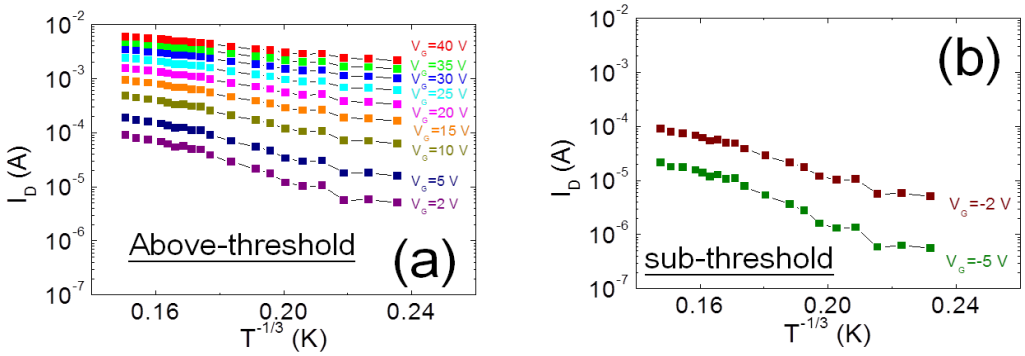

FIG. 3. Plot of logarithm of drain current (I_D) vs. $T^{-1/3}$ at various operation regions for ZTO TFT, (a) above-threshold ($V_G > V_{TH}$= -1.35 V), (b) sub-threshold (V_G< -1.35 V).

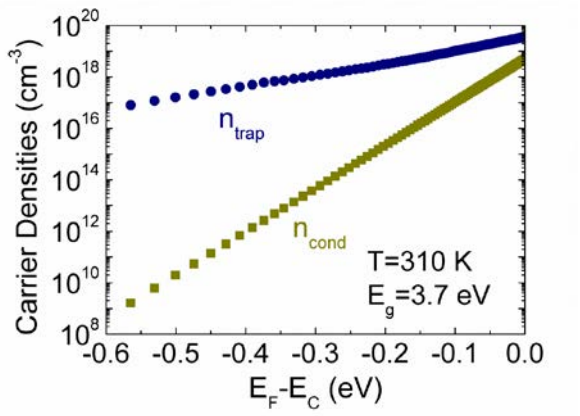

FIG. 4. Plot of conduction carrier density and trapped carrier density of ZTO TFT at 310K as a function of E_F-E_C.

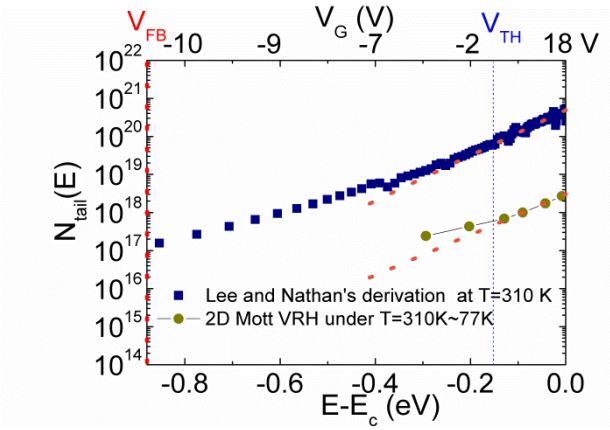

FIG. 5. The distribution of the density of localized tail states vs. $E-E_C$ in ZTO TFT, extracted using Lee and Nathan's derivation and 2D Mott's variable range hopping method. The dash line indicates the exponential profile of density of localized tail states, which follows $N_{tail}(E)=N_{tc}\exp[E-E_C)/kT_t]$.